Hindawi Publishing Corporation
Journal of Nanomaterials
Volume 2010, Article ID 935146, 5 pages
doi:10.1155/2010/935146

Review Article

Free Volumes Associated with Sintering in Gadolinium Doped Ceria Solid Solutions

Tomomi Kosaka[1] and Kiminori Sato[2]

[1] *Department of Chemistry, Tokyo Gakugei University, Koganei, Tokyo 184-8501, Japan*
[2] *Department of Environmental Sciences, Tokyo Gakugei University, Koganei, Tokyo 184-8501, Japan*

Correspondence should be addressed to Tomomi Kosaka, tkosaka@u-gakugei.ac.jp

Received 6 July 2010; Accepted 13 September 2010

Academic Editor: Ping Xiao

Gadolinium-doped ceria (GDC) solid solution prepared by the oxalate coprecipitation method is investigated by X-ray diffraction (XRD), complex impedance analysis, and positron lifetime spectroscopy. XRD reveals an expansion of GDC lattice constant by doping gadolinium into a ceria host crystal, in agreement with an oxygen vacancy model. The ionic conductivity of GDC measured at 773 K in air is two orders of magnitude higher than that of undoped ceria. Positron lifetime spectroscopy reveals the presence of vacancy-sized free volumes and nanovoids in interfaces among crystallites. It is found that the vacancy-sized free volumes shrink with increasing sintering temperatures. In the present paper, recent advances in the studies of GDC by XRD, complex impedance measurement, and positron lifetime spectroscopy are reviewed to gain an insight into the sintering mechanism.

1. Introduction

Ceria-based solid solution has drawn attention for decades as a candidate for fuel cell electrolytes due to their high ionic conductivity at intermediate temperatures [1–6]. Doping trivalent rare-earth oxides into ceria creates oxygen vacancies due to charge compensation. The type and composition of the rare-earth oxides greatly affect the physical properties of ceria solid solutions such as a density, ionic conductivity, and lattice constant [7]. Gd_2O_3 is the most promising rare-earth oxide since the association enthalpy between Gd^{3+} ion and oxygen vacancy is small resulting in high ionic conductivity on oxygen.

It has been suggested that highly densified ceria-based solid solution produces excellent oxygen ionic conductivity. In principle, high temperature sintering over 1573 K is required for GDC to achieve a density more than 90% with less open porosity. Such high temperature causes a replacement from CeO_2 to Ce_2O_3, which leads to produce microcracks along with the degradation of conduction efficiency. Takamura et al. [8] observed the enhancement of electric conductivity under gigapascal pressure regimes for acceptor-doped ceria nanoparticles. They attributed the enhancement of electric conductivity under the high pressure to the densification of granular particles.

Positrons preferentially localize at atomic disorder as, for example, grain boundary [9], and provide the information on local atomic structures at annihilation sites [10, 11]. Some experiments by positron annihilation spectroscopy predicted the presence of vacancy-like defects and larger free volumes associated with interfaces among crystallites for zirconia-based materials [12, 13]. Garay et al. [13] proposed that defects in negatively charged grain-boundary space region correspond to positron trapping sites, since positrons are not trapped by positively charged spaces such as oxygen vacancies.

Here, recent advances [14] in the study of GDC by XRD, complex impedance measurement, and positron lifetime spectroscopy are reviewed. We focus on the evolution of local atomic structures at interfaces upon sintering to gain an insight into the densification mechanism.

2. Experimental

2.1. Sample Preparation. GDC was prepared by the oxalate coprecipitation method [15]. Starting materials employed

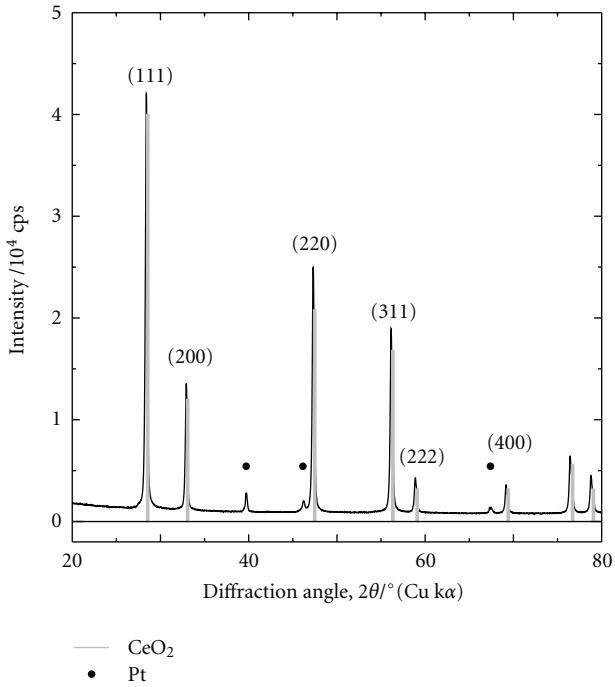

Figure 1: XRD pattern of GDC sintered at 1073 K for 6 hours in air. For comparison, the data of CeO_2 taken from JCPDS No. 34-394 is added.

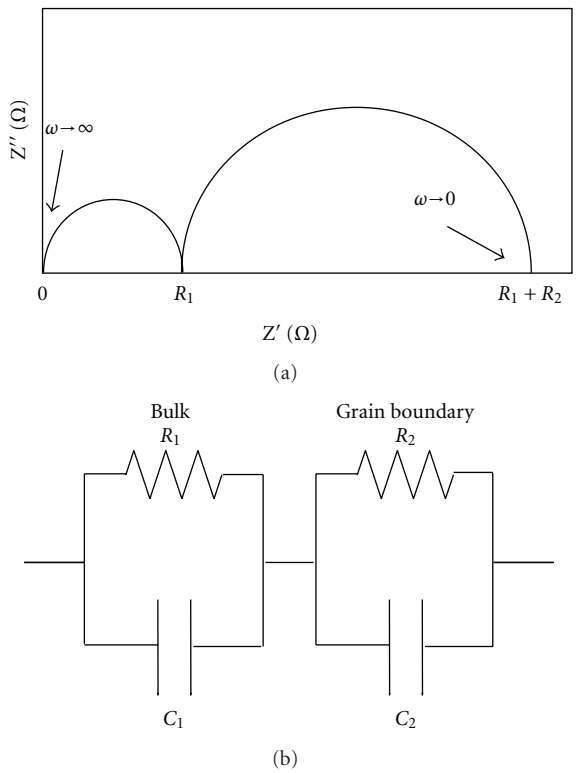

Figure 2: Illustrations of (a) the Nyquist plot of typical complex impedance for GDC, and (b) equivalent electrical circuit for interpreting complex impedance of GDC.

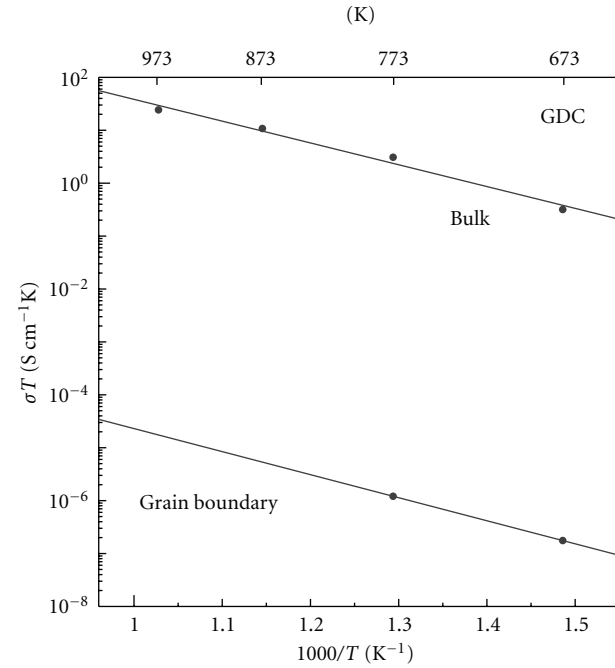

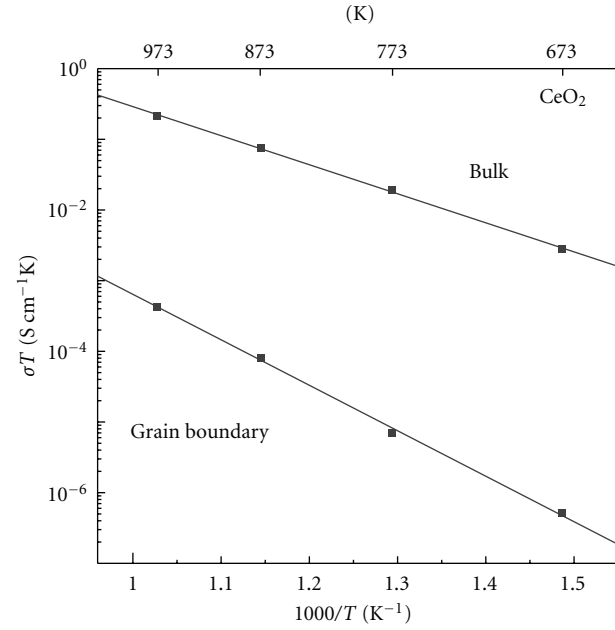

Figure 3: Arrhenius plots of ionic conductivity calculated from the bulk and grain boundary resistance for GDC and CeO_2.

were $Ce(NO_3)_3 \cdot 6H_2O$, $Gd(NO_3)_3 \cdot 6H_2O$, and $H_2C_2O_4 \cdot 2H_2O$. All reagents were purchased from Wako Pure Chemical industries LTD. The cerium and gadolinium nitrate solutions (0.2 mol/l) were mixed at a gadolinium molar ratio of approximately 0.2. The mixed solution was dropped into a stirred oxalic acid solution (0.4 mol/l) to produce an oxalate coprecipitate. The coprecipitate filtered was washed with ion exchanged water in several times, and then dried at 313 K for 8 hours. The oxalate coprecipitate was decomposed to GDC

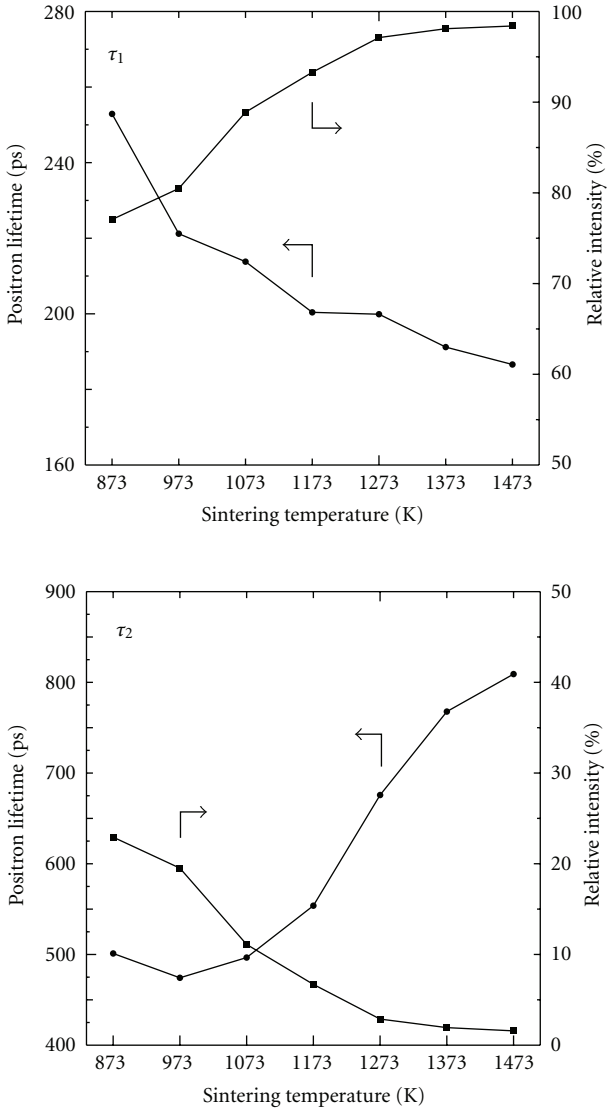

FIGURE 4: Positron lifetimes (τ_1 and τ_2) and their relative intensities (I_1 and I_2) as a function of sintering temperatures.

by calcining at 873 K in air for 1 hour. The GDC powder was uniaxially pressed into a pellet with 10 mm diameter and 2 mm thickness under the pressure of 20 MPa. The GDC pellets were sintered in the temperature range from 873 K to 1273 K for 6 hours in air.

2.2. Characterization. The lattice parameters of GDC were calculated from diffracted peaks measured by Cu Kα X-ray diffractometer (Ultima IV, Rigaku corp.) operated at 40 kV, 50 mA. The scattering angles were calibrated using Si powder (NIST 640c). The crystallite size was estimated from (111) diffraction peak by Scherrer's equation. The bulk density was measured by the Archimedes method using ion exchanged water. The Pt electrodes were formed on the both sides of GDC pellet by heating at 1473 K using Pt paste (Tanaka Kikinzoku TR-7070). The oxygen ionic conductivity was measured in air in the temperature range from 673 K to 973 K by the complex impedance analyzer (Princeton applied research corp. VersaSTAT3) in the frequency range from 100 μHz to 1 MHz. The impedance data was analyzed using ZView software (Scribner Associates).

2.3. Positron Lifetime Spectroscopy. Positron lifetime spectroscopy with a digital oscilloscope-based spectrometer was performed at room temperature. The positron source (^{22}Na), sealed in a thin foil of Kapton, was mounted in a sample-source-sample sandwich. Positron lifetime spectra ($\sim 10^6$ coincidence counts) were recorded with a time resolution of 180 ps full-width at half-maximum (FWHM). The data were numerically analyzed using the POSITRONFIT code [16].

3. Results and Discussion

Figure 1 shows the XRD pattern of GDC sintered at 1073 K for 6 hours in air. The XRD pattern indicates that GDC has a fluorite type structure without any other phases. The peaks denoted as Pt indicate the diffraction from a sample holder. All peaks of GDC are shifted to a low angle with respect to corresponding ones of CeO_2 (denoted as solid bar) indicating the expansion of interplanar spacing for GDC by Gd doping. The lattice parameter calculated for GDC was 0.54245 ± 0.00006 nm. Hong and Virkar [7] reported that the lattice constant a of GDC is given by the following equation"

$$a = \frac{4}{\sqrt{3}}[xr_1 + (1-x)r_2 + (1-0.25x)r_3 + 0.25xr_4] \times 0.9971, \quad (1)$$

where x, r_1, r_2, r_3, and r_4 are the concentration of gadolinium ion, the radii of the gadolinium ion (0.1053 nm), cerium ion (0.097 nm), oxygen ion (0.138 nm), and the oxygen vacancy (0.1164 nm), respectively. The factor, 0.9971, was introduced for correcting the discrepancy between the lattice constant measured for pure ceria (0.5411 nm; JCPDS No.34-394) and calculated by (1) with $x = 0$. Inserting the lattice constant calculated from XRD peaks into (1) yields the Gd composition of ~0.1969. In the case of our GDC sintered at 1273 K, the relative density is 80%. It may be thus unsuitable to directly discuss the structure of GDC with the results of Archimedes method. Based on the results of XRD reported above and experimental evidence confirming the oxygen vacancy model [17], we conclude that substitution of Ce^{4+} with Gd^{3+} partially occurs and oxygen vacancies are successfully formed.

The typical complex impedance of samples consists of two semicircles in the Nyquist plot as illustrated in Figure 2(a). The impedance arc can be thus interpreted with equivalent electrical circuits (see Figure 2(b)). One semicircle in the high frequency range and the other in the low frequency range may correspond to oxygen migration in the bulk and across grain boundaries, respectively. Figure 3 shows Arrhenius plots of the ionic conductivity calculated from the resistance of the bulk and grain boundary for GDC

and CeO_2. The conductivity of grain boundary is lower than that of bulk in both samples. The bulk conductivity of GDC at 773 K is estimated to be 4.0×10^{-3} Scm^{-1}, which is 160 times higher than that of CeO_2. The activation energy for bulk conductivity in GDC was 78.9 kJ/mol, which is close to the value (75 kJ/mol) reported by Faber et al. [18]. The activation energies of grain boundary for GDC and CeO_2 are relatively higher than that of bulk, suggesting that the diffusion of oxygen ion is affected by the local structural disorders at grain boundaries.

Figure 4 shows the results of positron lifetime spectroscopy for GDC. Prior to sintering, two components τ_1 ($\sim$260 ps) and τ_2 ($\sim$500 ps) corresponding to a vacancy-sized free volume and nanovoid were obtained with their relative intensities I_1 ($\sim$80%) and I_2 ($\sim$20%), respectively. The average size of GDC crystallite evaluated from XRD 111 peak broadening using Scherrer's equation is 12.8 nm before sintering, which is by far smaller than the typical positron diffusion length in solids ($\sim$300 nm) [19]. Positrons implanted in GDC crystallite can thus efficiently diffuse out and annihilate at interfaces among crystallites. We therefore conclude that the vacancy-sized free volumes and nanovoids are present at interfaces among crystallites. Similar observation was reported for yttria-stabilized zirconia by Čížek et al. [12].

With increasing temperatures the positron lifetime τ_1 decreases and its relative intensity I_1 increased, signifying a shrinkage of vacancy-sized free volumes together with sintering. The lifetime τ_2 and its relative intensity I_2 exhibit the opposite tendency to those of vacancy-sized free volume. The vacancy-sized free volumes got dominant at the sintering temperature of 1473 K, while the nanovoids almost disappear. The results suggest that a substantial increase of local electron density at interfaces among crystallites occurs as a result of sintering and the sintering process of GDC follows the kinetics of vacancy-sized free volumes and nanovoids at interfaces among crystallites.

4. Conclusion

Recent advance in the studies of GDC by XRD, complex impedance measurement, and positron lifetime spectroscopy were reviewed to gain an insight into the sintering mechanism. XRD revealed that the fluorite structure with oxygen vacancies for GDC, indicating that gadolinium is successfully doped into cerium oxide. The bulk ionic conductivity of GDC sintered at 773 K for 6 h in air is 4.0×10^{-3} S/cm, which is 160 times higher than that of CeO_2. The result indicates that the oxygen vacancies have an influence on the bulk ionic conductivity sufficiently. Positron lifetime spectroscopy revealed the presence of vacancy-sized free volumes and nanovoids, of which the kinetics is associated with sintering.

Acknowledgment

The authors would like to thank Professor K. Shinozaki (Tokyo Institute of Technology) for experimental assistance in the complex impedance measurement.

References

[1] H. Yahiro, T. Ohuchi, K. Eguchi, and H. Arai, "Electrical properties and microstructure in the system ceria-alkaline earth oxide," *Journal of Materials Science*, vol. 23, no. 3, pp. 1036–1041, 1988.

[2] D. L. Maricle, T. E. Swarr, and S. Karavolis, "Enhanced ceria—a low-temperature SOFC electrolyte," *Solid State Ionics*, vol. 52, no. 1–3, pp. 173–182, 1992.

[3] H. Inaba and H. Tagawa, "Ceria-based solid electrolytes," *Solid State Ionics*, vol. 83, no. 1-2, pp. 1–16, 1996.

[4] M. Gödickemeier, K. Sasaki, L. J. Gauckler, and I. Riess, "Electrochemical characteristics of cathodes in solid oxide fuel cells based on ceria electrolytes," *Journal of the Electrochemical Society*, vol. 144, no. 5, pp. 1635–1646, 1997.

[5] K. R. Reddy and K. Karan, "Sinterability, mechanical, microstructural, and electrical properties of gadolinium-doped ceria electrolyte for low-temperature solid oxide fuel cells," *Journal of Electroceramics*, vol. 15, no. 1, pp. 45–56, 2005.

[6] L. D. Jadhav, M. G. Chourashiya, K. M. Subhedar, A. K. Tyagi, and J. Y. Patil, "Synthesis of nanocrystalline Gd doped ceria by combustion technique," *Journal of Alloys and Compounds*, vol. 470, no. 1-2, pp. 383–386, 2009.

[7] S. J. Hong and A. V. Virkar, "Lattice parameters and densities of rare-earth oxide doped ceria electrolytes," *Journal of the American Ceramic Society*, vol. 78, no. 2, pp. 433–439, 1995.

[8] H. Takamura, J. Kobayashi, N. Takahashi, and M. Okada, "Electrical conductivity of ceria nanoparticles under high pressure," *Journal of Electroceramics*, vol. 22, no. 1–3, pp. 24–32, 2009.

[9] K. Sato, H. Murakami, W. Sprengel, H.-E. Schaefer, and Y. Kobayashi, "Nanocrystallization mechanism of amorphous Fe78 B13 Si9," *Applied Physics Letters*, vol. 94, no. 17, Article ID 171904, 2009.

[10] K. Sato, F. Baier, W. Sprengel, R. Würschum, and H.-E. Schaefer, "Study of an order-disorder phase transition on an atomic scale: the example of decagonal Al-Ni-Co quasicrystals," *Physical Review Letters*, vol. 92, no. 12, Article ID 127403, 2004.

[11] K. Sato, D. Shanai, Y. Hotani et al., "Positronium formed by recombination of positron-electron pairs in polymers," *Physical Review Letters*, vol. 96, no. 22, Article ID 228302, 2006.

[12] J. Čížek, O. Melikhova, J. Kuriplach, I. Prochazka, T. E. Konstantinova, and I. A. Danilenko, "Defects in yttria-stabilised zirconia: a positron annihilation study," *Physica Status Solidi C*, vol. 4, no. 10, pp. 3847–3850, 2007.

[13] J. E. Garay, S. C. Glade, P. Asoka-Kumar, U. Anselmi-Tamburini, and Z. A. Munir, "Characterization of densified fully stabilized nanometric zirconia by positron annihilation spectroscopy," *Journal of Applied Physics*, vol. 99, no. 2, Article ID 024313, pp. 1–7, 2006.

[14] S. Ohta, T. Kosaka, and K. Sato, "Study of Gadolinium-doped cerium oxide by XRD, TG-DTA, impedance analysis, and positron lifetime spectroscopy," *Journal of Physics: Conference Series*, vol. 255, Article ID 012043, 2010.

[15] S. Sameshima, H. Ono, K. Higashi, K. Sonoda, and Y. Hirata, "Microstructure of rare-earth-doped ceria prepared by oxalate coprecipitation method," *Journal of the Ceramic Society of Japan*, vol. 108, no. 11, pp. 985–988, 2000.

[16] P. Kirkegaard and M. Eldrup, "Positronfit extended: a new version of a program for analysing position lifetime spectra," *Computer Physics Communications*, vol. 7, no. 7, pp. 401–409, 1974.

[17] T. H. Esell and S. N. Flengas, "The electrical properties of solid oxide electrolytes," *Chemical Reviews*, vol. 70, pp. 339–376, 1970.

[18] J. Faber, C. Geoffroy, A. Roux, A. Sylvestre, and P. Abélard, "A Systematic investigation of the dc electrical conductivity of rare-earth doped ceria," *Applied Physics A Solids and Surfaces*, vol. 49, no. 3, pp. 225–232, 1989.

[19] T. E. M. Staab, R. Krause-Rehberg, and B. Kieback, "Positron annihilation in fine-grained materials and fine powders—an application to the sintering of metal powders," *Journal of Materials Science*, vol. 34, no. 16, pp. 3833–3851, 1999.